Visual Neuroscience (2004), **21**, 725–738. Printed in the USA.

DOI: 10.1017/S0952523804045079

Decorrelation of neural activity during fixational instability: Possible implications for the refinement of V1 receptive fields

MICHELE RUCCI[1] AND ANTONINO CASILE[2]

[1]Department of Cognitive and Neural Systems, Boston University, Boston Massachusetts
[2]Laboratory for Action Representation and Learning, Department of Cognitive Neurology, University Clinic, Tübingen, Germany

(RECEIVED April 20, 2004; ACCEPTED June 10, 2004)

Abstract

Early in life, visual experience appears to influence the refinement and maintenance of the orientation-selective responses of neurons in the primary visual cortex. After eye opening, the statistical structure of visually driven neural responses depends not only on the stimulus, but also on how the stimulus is scanned during behavior. Modulations of neural activity due to behavior may thus play a role in the experience-dependent refinement of cell response characteristics. To investigate the possible influences of eye movements on the maturation of thalamocortical connectivity, we have simulated the responses of neuronal populations in the lateral geniculate nucleus (LGN) and V1 of the cat while images of natural scenes were scanned in a way that replicated the cat's oculomotor activity. In the model, fixational eye movements were essential to attenuate neural sensitivity to the broad correlational structure of natural visual input, decorrelate neural responses, and establish a regime of neural activity that was compatible with a Hebbian segregation of geniculate afferents to the cortex. We show that this result is highly robust and does not depend on the precise characteristics of the model.

Keywords: Orientation selectivity, Striate cortex, Microsaccade, Ocular drift, Computational model

Introduction

The developmental origins of the orientation-selective responses of neurons in the primary visual cortex (V1) have been intensively investigated. Most studies agree that while the initial maturation of orientation selectivity does not rely on external visual experience, visual experience becomes crucial in a later phase of development for the maintenance and further refinement of response selectivity (Pettigrew, 1974; Buisseret & Imbert, 1976; Sherk & Stryker, 1976; Fregnac & Imbert, 1978; Albus & Wolf, 1984; Hirsch, 1985; Chapman & Stryker, 1993; Crair et al., 1998). In this critical period, the statistical structure of visual stimulation influences the maturation of orientation-selective responses, as shown by experiments with chronic exposure to abnormal visual input, as for example with kittens and ferrets raised in environments containing only edges with a specific orientation (Hirsch & Spinelli, 1970; Blakemore & Van Sluyters, 1975; Stryker et al., 1978; Sengpiel, 1999) or with their lid sutured to experience only diffuse light (White et al., 2001).

Although the precise role of neural activity in the maturation of orientation selectivity remains controversial (Stryker & Harris, 1986; Fregnac et al., 1992; Chapman & Stryker, 1993; Weliki & Katz, 1997; for a recent review see Miller et al., 1999), many experimental data are consistent with a correlation-based mechanism of plasticity (Stent, 1973; Changeux & Danchin, 1976) that operates initially on spontaneous neural activity and later on visually driven neuronal responses. According to the Hebbian hypothesis, the stabilization of synchronously firing afferents onto common postsynaptic neurons is responsible for the segregation of geniculate afferents from ON- and OFF-center cells into the adjacent, oriented subregions that, in the receptive fields of V1 simple cells, respond to bright and dark stimuli (Hubel & Wiesel, 1962; Zahs & Stryker, 1988; Chapman et al., 1991; Reid & Alonso, 1995; Ferster et al., 1996; Chung & Ferster, 1998). Modeling studies that simulated spontaneous activity have shown the plausibility of this proposal before eye opening (Linsker, 1986; Miyashita & Tanaka, 1992; Miller, 1994). However, given that the statistical structure of endogenous spontaneous activity differs profoundly from that of visually driven responses, it is not clear how the same mechanism of synaptic plasticity could account for both the initial segregation of thalamic afferents and their later refinement. In particular, the broad spatial correlations that characterize natural scenes would tend to co-activate retinal and geniculate cells with similar polarity at large separations in the visual field, a result that appears incompatible with a Hebbian segregation of geniculate afferents.

Address correspondence and reprint requests to: Michele Rucci, Department of Cognitive and Neural Systems, Boston University, 677 Beacon Street, Boston MA 02215, USA. E-mail: rucci@cns.bu.edu

A potential resolution of this problem could lie in the fact that, after eye opening, the spatiotemporal structure of the signals entering the eyes depends not only on the statistical characteristics of the visual scene, but also on the movement performed by the animal during the acquisition of visual information. Modulations of neural responses due to motor behavior could influence activity-dependent synaptic modifications. In particular, oculomotor behavior, with its direct impact on the sampling of visual information, may well affect visual development. Eye movements are always present during natural vision, as small movements occur even while the eye is fixating on a target (Ditchburn, 1973; Steinman et al., 1973). Interestingly, impairments in the plasticity underlying ocular dominance (Freeman & Bonds, 1979; Singer & Raushecker, 1982) and orientation selectivity (Buisseret et al., 1978; Buisseret, 1995) have been reported in kittens when eye movements are prevented.

This study builds upon our previous work on modeling neural activity in the lateral geniculate nucleus (LGN) of the cat (Rucci et al., 2000). In these previous simulations, the second-order statistical structure of neural activity during the jittering of visual fixation was found to match the average spatial organization of simple cell receptive fields. In this study, we investigate the possible impact of these short-lived patterns of synchronous thalamic activity on the long-term correlation and covariance between thalamic and cortical cells. Based on the results of our simulations, we suggest that the normal instability of visual fixation may play an important role in the refinement and maintenance of thalamocortical connectivity.

Materials and methods

In the experiments described in this paper, the activity of cells in the LGN and V1 of the cat was simulated while images of natural scenes were presented during oculomotor behavior. Some elements of the simulations have been described in a previous publication (Rucci et al., 2000). This section focuses on the elements of the model that are novel to this work or that differed from our previous simulations.

Modeling neural activity

Neuronal responses to visual stimuli were modeled by means of spatiotemporal filters that replicated the changes in a cell's instantaneous firing rate with respect to the level of spontaneous activity. Independent filters were used to model LGN and V1 neurons. For both geniculate and cortical neurons, models were composed of the cascade of two stages, with a second nonlinear stage that operated on the result of the convolution between the input signal I (the input to the retina during oculomotor activity) and the cell spatiotemporal kernel K. The mean instantaneous firing rate $\gamma(t)$ of a cell with a receptive field at position (x, y) of the visual field was given by

$$\begin{aligned}\gamma(t) &= \mathcal{N}\{K(x,y,t) * I(x,y,t)\} \\ &= \mathcal{N}\left\{\int_0^t \int_{-\infty}^{\infty}\int_{-\infty}^{\infty} K(x',y',t') \right. \\ &\qquad \left. \times I(x-x', y-y', t-t')\,\mathrm{d}x'\,\mathrm{d}y'\,\mathrm{d}t'\right\}, \qquad (1)\end{aligned}$$

where $\mathcal{N}\{\cdot\}$ indicates a different nonlinear operator for thalamic and cortical cells.

Lateral geniculate nucleus

Simulated geniculate neurons included ON- and OFF-center nonlagged X cells with receptive fields located between 5 deg and 25 deg of visual eccentricity. The activity of these cells was simulated as in Rucci et al. (2000), following the model proposed by Cai et al. (1997). In brief, the spatiotemporal kernel of a geniculate unit α, $K_\alpha(x, y, t)$, was modeled as the sum of two terms that represented the contributions from the center and periphery of the receptive field. Each term was separable in its spatial and temporal components, that is $K_\alpha(x, y, t) = F^c_\alpha(x, y)G^c_\alpha(t) - F^s_\alpha(x, y)G^s_\alpha(t)$. For both the center and the surround, the spatial element $F_\alpha(x, y)$ was a two-dimensional (2D) Gaussian function. Spatial parameters were adjusted according to the visual eccentricity of the cell following neurophysiological data (Linsenmeier et al., 1982). The temporal element $G(t)$ was modeled as the difference of two gamma functions (Deangelis et al., 1993*a*; Cai et al., 1997). The second stage of the model [the nonlinear operator $\mathcal{N}\{\cdot\}$ in eqn. (1)] rectified the output of the linear stage by eliminating responses below a specified threshold θ. In the experiments, θ was adjusted to eliminate 75% of the range of negative responses. A modulation of geniculate activity occurred in the correspondence of each saccade. An initial suppression of activity with a peak of 10% gradually reversed to a 20% facilitation with a peak occurring 100 ms after the end of the saccade (Lee & Malpeli, 1998). Simulations with different parameters showed that the results are largely unaffected by the percentage of rectification and the degree of saccadic modulation (data not shown).

V1 simple cells

Ten simple cells were modeled. The linear kernels $K_\eta(x, y, t)$ of these cells were assumed to be separable in their spatial and temporal components, that is, $K_\eta(x, y, t) = F_\eta(x, y)G_\eta(t)$. Spatial kernels were modeled by Gabor functions:

$$\begin{aligned}F_\eta(x,y) &= A\cos(2\pi\omega_0 x + \alpha) \\ &\quad \times \left[\exp - \left(\frac{(x\cos\phi - y\sin\phi)^2}{2\sigma_x^2}\right)\right. \\ &\quad \left. - \left(\frac{(x\sin\phi + y\cos\phi)^2}{2\sigma_y^2}\right)\right],\end{aligned}$$

where A is the amplitude, σ_x and σ_y are the standard deviations of the elliptic Gaussian, ω_0 and α are the angular velocity and phase of the plane wave, and ϕ is the angle between the plane wave and the Gaussian axes. The parameters were adjusted individually for each simulated cell following the neurophysiological data of Jones and Palmer (1987*a*,*b*). The temporal profile $G_\eta(t)$ was modeled as the difference of two gamma functions, in a similar way to the profile of geniculate cells. In this paper, we use ON and OFF labels to indicate the regions of simple cell receptive fields that are excited respectively by bright and dark stimuli.

In the simulations of Figs. 2–6, the responses of simple cells were modeled linearly by means of the spatiotemporal convolution of the unit kernels and the input signal to the retina. That is, in these simulations $\mathcal{N}\{\cdot\}$ in eqn. (1) was equal to the identity function. In the simulations of Figs. 8 and 9, the nonlinear operator $\mathcal{N}\{\cdot\}$ in eqn. (1) modeled the fast decay in the responses of cortical

cells to stationary stimuli (Ikeda & Wright, 1975; Tolhurst et al., 1980; Deangelis et al., 1993*b*). This faster than linear adaptation may have important effects on neuronal responses during oculomotor activity, when abrupt changes in the visual stimulus introduced by saccades are followed by periods of fixation in which the stimulus tends to vary more gradually. Previous studies have modeled this nonlinear adaptation of V1 cells by mechanisms of short-term synaptic depression operating on simulated train of spikes [see for example Abbott et al. (1997); Tsodyks & Markram (1997)]. These models were not applicable in our simulations because of the intense computational load that originated from the need for massive statistical averaging. For this reason, we modeled the nonlinear decay of V1 responses directly on the mean instantaneous firing rate. This model, which decreased simulation time by a factor of 50, consisted of an adaptive circuit composed of the parallel of a capacitance C and a conductance G. The conductance varied as a function of the cell activity $\eta(t)$ as shown in eqn. (2). The circuit received input current H proportional to the output of the convolution in eqn. (1) [i.e. $H(t) = K(x, y, t) * I(x, y, t)$], and produced a mean instantaneous firing rate proportional to the voltage $\eta(t)$ across the conductor:

$$\begin{cases} C\dfrac{\mathrm{d}\eta(t)}{\mathrm{d}dt} = H(t) - \eta(t)G, \\ \dfrac{\mathrm{d}G}{\mathrm{d}t} = \lambda(\eta(t) - \eta_0), \end{cases} \tag{2}$$

where η_0 is a resting potential that defines the level of spontaneous activity and λ is a constant. In the presence of a steady input, $H(t) = H_0$, $\eta(t)$ declines while G increases until the stationary values $\eta_\infty = \eta_0$ and $G_\infty = H_0/\eta_0$ are reached. This model was designed to replicate the time course of firing rates of V1 units. It is not meant to compose a biophysical model of the cell membrane. For input currents in the range (0.4–0.6), this adaptive circuit well approximates the firing rate predicted by models of short-term synaptic plasticity. The result of the spatiotemporal convolution in eqn. (1) was scaled to fit within this range, and the values of the parameters were estimated empirically by fitting neurophysiological data and the output of spike-based models of short-term synaptic depression (Varela et al., 1997; Tsodyks et al., 1998). Typical values used in the simulations were $C = 100$ pF, $\lambda = 55(\mathrm{As})^{-1}$, and $\eta_0 = 0.2$ V.

Visual stimulation

A database of 82 pictures of natural scenes (van Hateren & van der Schaaf, 1998) was used in the experiments. These images consisted of 1536×1024 pixels, spanning an area of approximately 25 by 17 deg of the visual field. The radial mean of the power spectrum was best interpolated by $S(w) = Aw^{-1.85}$, which is consistent with the results of other studies (Ruderman & Bialek, 1994). The oculomotor behavior of the cat was modeled as in Rucci et al. (2000) and consisted of saccades and fixational eye movements. Fixational instability included small saccades, ocular drifts, and tremor.

Spontaneous activity was modeled on the basis of the Mastronarde (1983) data. Mastronarde's estimate of the correlation between the activity of two X cells in the retina at a relative distance d was approximated by the function $c_e = 15 - 3.75 s_e(d)$, where e is the visual eccentricity and $s_e(d)$ indicates the distance expressed in spacings [$s_e(d) = 0.186 \cdot d \cdot \sqrt{N_e}$, where N_e is the cell density at eccentricity e]. This measurement provides a first-order approximation of spontaneous activity and neglects sources of correlation other than the spatial organization of cell receptive fields.

Data collection and analysis

To allow a direct comparison between the spatial organization of V1 receptive fields and the structure of covarying activity, for each simulated simple cell η we evaluated a correlation difference map, $C_\eta^D(x, y)$, that summarized the levels of covariance between the response of η and those of a population of 648 LGN units. Geniculate units were arranged in two 18 by 18 grids of ON- and OFF-center cells with receptive fields at evenly spaced locations within the receptive field of η. As illustrated in Fig. 1, the value at each location (x, y) of the map represents the difference in the levels of covariance between the activity of the V1 unit, $\eta(t)$, and those of the two ON- and OFF-center LGN units with receptive fields centered at location (x, y) within η's receptive field, $\alpha_{xy}^{\mathrm{ON}}(t)$ and $\alpha_{xy}^{\mathrm{OFF}}(t)$:

$$\begin{aligned} C_\eta^D = \langle [\eta(t) - \bar{\eta}][\alpha_{xy}^{\mathrm{ON}}(t) - \bar{\alpha}_{xy}^{\mathrm{ON}}] \rangle \\ - \langle [\eta(t) - \bar{\eta}][\alpha_{xy}^{\mathrm{OFF}}(t) - \bar{\alpha}_{xy}^{\mathrm{OFF}}] \rangle, \end{aligned} \tag{3}$$

where the averages are evaluated over time and space (the database of natural images). A positive value in $C_\eta^D(x, y)$ indicates that the simple cell η tends to covary more strongly with an ON-center, rather than an OFF-center, LGN neuron with receptive field at a separation (x, y). The opposite occurs for a negative value of $C_\eta^D(x, y)$.

Second-order statistics were evaluated by simulating neural responses over 120 eye trajectories for each input image. In the experiments with sustained visual fixation, each image was examined for a total of 552 s with each fixation lasting 4.6 s. In the experiments that included large saccades, each image was examined for a period of 792 s, and the duration of each trial was 6.6 s. In these experiments, the analysis of covarying activity during visual fixation was obtained by selecting fixations with duration longer than 300 ms and by removing the initial transitory 150 ms from saccade onset. In all experiments, the initial 0.6 s of simulated activity were discarded in each trial from the statistical analysis to avoid artifacts due to the onset of stimulation.

In some cases, a first-order approximation of the correlation difference maps was evaluated by considering LGN and V1 units as linear filters. Correlation difference maps were estimated by means of the spatiotemporal correlation $r(x,y,t)$ of the input [the correlation between the luminances of pixels at a separation (x, y) measured at a time lag t], or equivalently the input power spectrum $R(\mathbf{w}, f)$, where $\mathbf{w}$ and f indicate spatial and temporal frequencies. Under the assumption of linearity, the correlation $r_{\eta\alpha}(x, y, t)$ between a cortical unit η and a ON-center geniculate unit α can be evaluated by the inverse Fourier transform of the product of the power spectrum of the input signal I and the Fourier transforms of the spatial kernels of cortical and geniculate cells (see for example, Bendat & Piersol, 1986). With the simplifying assumption that all geniculate cells are characterized by equal values of mean activity $\bar{\alpha}$, the correlation difference map was given by

$$C_\eta^{\mathrm{D}}(x, y) = r_{\eta\alpha}(x, y, 0) - \bar{\eta}\bar{\alpha}, \tag{4}$$

where $\bar{\eta}$ is the mean of the response of the cortical unit.

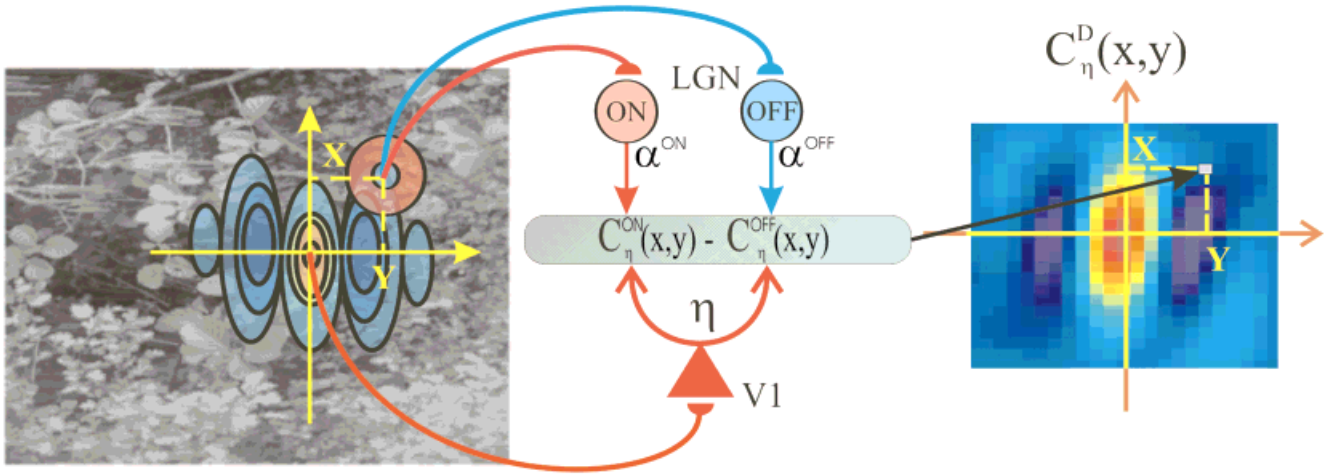

Fig. 1. A correlation difference map C^D_η summarizes the spatial structure of covarying activity between a selected cortical cell η and a population of LGN neurons with receptive fields in different retinotopic positions. The value at each point (x, y) in the map is given by the difference of the levels of covariance between the activity of η and the responses of the ON- and OFF-center LGN neurons with receptive fields at a distance (x, y) from the center of η's receptive field. Positive (negative) values in the correlation difference map are locations within the receptive field of η in which the activity of the cortical unit covaries more closely with the responses of ON-center (OFF-center) rather than OFF-center (ON-center) LGN units. For clarity, only one of the two overlapping geniculate receptive fields is shown in the panel on the left.

Results

The hypothesis that a Hebbian mechanism of synaptic plasticity regulates the stabilization of geniculate afferents to V1 simple cells implies a consistency between the second-order statistics of thalamocortical activity and the spatial organization of simple cell receptive fields. That is, synchronous activity is required between an LGN neuron and a V1 simple cell if the receptive field of the geniculate neuron overlaps one of the ON or OFF subregions in the cortical receptive field with a sign matching its polarity (ON- or OFF-center). To quantitatively investigate the existence of such consistency, we simulated the responses of neuronal populations in the LGN and V1 and examined the structure of thalamocortical activity under different viewing conditions. As explained in the Methods section, LGN and V1 neurons were modeled by means of independent spatiotemporal filters designed on the basis of neurophysiological data, and correlation difference maps were used to compare the structure of covarying activity to the spatial organization of the receptive fields of simulated V1 units.

Among the factors that affect the levels of covariance between thalamic and cortical responses, a first important element is the statistical structure of the input signals. Images of natural scenes are characterized by a low degree of spatial variability; that is, nearby pixels tend to possess on average similar intensity and color properties, as revealed by the broad shape of their spatial correlations (Field, 1987; Ruderman & Bialek, 1994). First, we investigated the possible impact of these input correlations on neural activity. Pictures of natural scenes were presented to the model and correlation difference maps were analyzed at steady state. No eye movements were present in these simulations. Fig. 2(a) shows the correlation difference maps measured for two simulated simple cells. Modeled LGN units replicated the responses of cells located around 17 deg of visual eccentricity. For both simple cells, a clear mismatch was present between the spatial organization of receptive fields and the correlation difference maps. This mismatch was particularly evident on the lateral subregions in the receptive fields, which were absent in the patterns of covarying activity.

The results obtained with static presentation of natural visual input for all ten simulated cortical cells are summarized in Fig. 2(b). The receptive field of these cells were modeled following the Jones and Palmer (1987*b*) neurophysiological data. The precise eccentricity of cell receptive fields was not given in these data, but both in the cat and in the monkey a large overlap is known to exist in the receptive-field characteristics of cells located at different angles of visual eccentricity (Wilson & Sherman, 1976; DeValois & DeValois, 1990). For this reason, in separate simulations, we analyzed the structure of covarying activity between the entire population of simulated V1 neurons and LGN units that replicated the responses of cells located at different angles of visual eccentricity. The consistency between patterns of covarying activity and spatial receptive fields was measured by the percentage of receptive-field area in which receptive-field subregions and correlation difference maps shared the same sign. As shown by the light bars in Fig. 2(b), at all simulated visual eccentricities, in approximately half of the cases cortical responses covaried strongly with LGN cells with the wrong polarity (ON- rather than OFF-center and *vice-versa*). The mean percentage of correct matching over all the simulated simple cells and all the examined angles of visual eccentricity was only 51%. Since for many simple cells the mismatch between patterns of covarying activity and receptive fields was particularly pronounced over the side lobes in the receptive fields, we evaluated a second, more specific index of consistency by restricting the analysis of sign matching to these lateral subregions. As shown by the dark bars in Fig. 2(b), matching percentages over the side lobes were low at all visual eccentricities, and the mean percentage of correct matching was only 18%. Thus, secondary subregions in the receptive fields of cortical cells were almost completely lost in the patterns of connectivity predicted by the correlation difference maps.

Fig. 2(c) provides a second comparison between the results of our simulations and neurophysiological data. In this case, the average width of the central lobe of V1 receptive fields measured in the cat striate cortex by Wilson and Sherman (1976) at several angles of visual eccentricity was compared to the width predicted

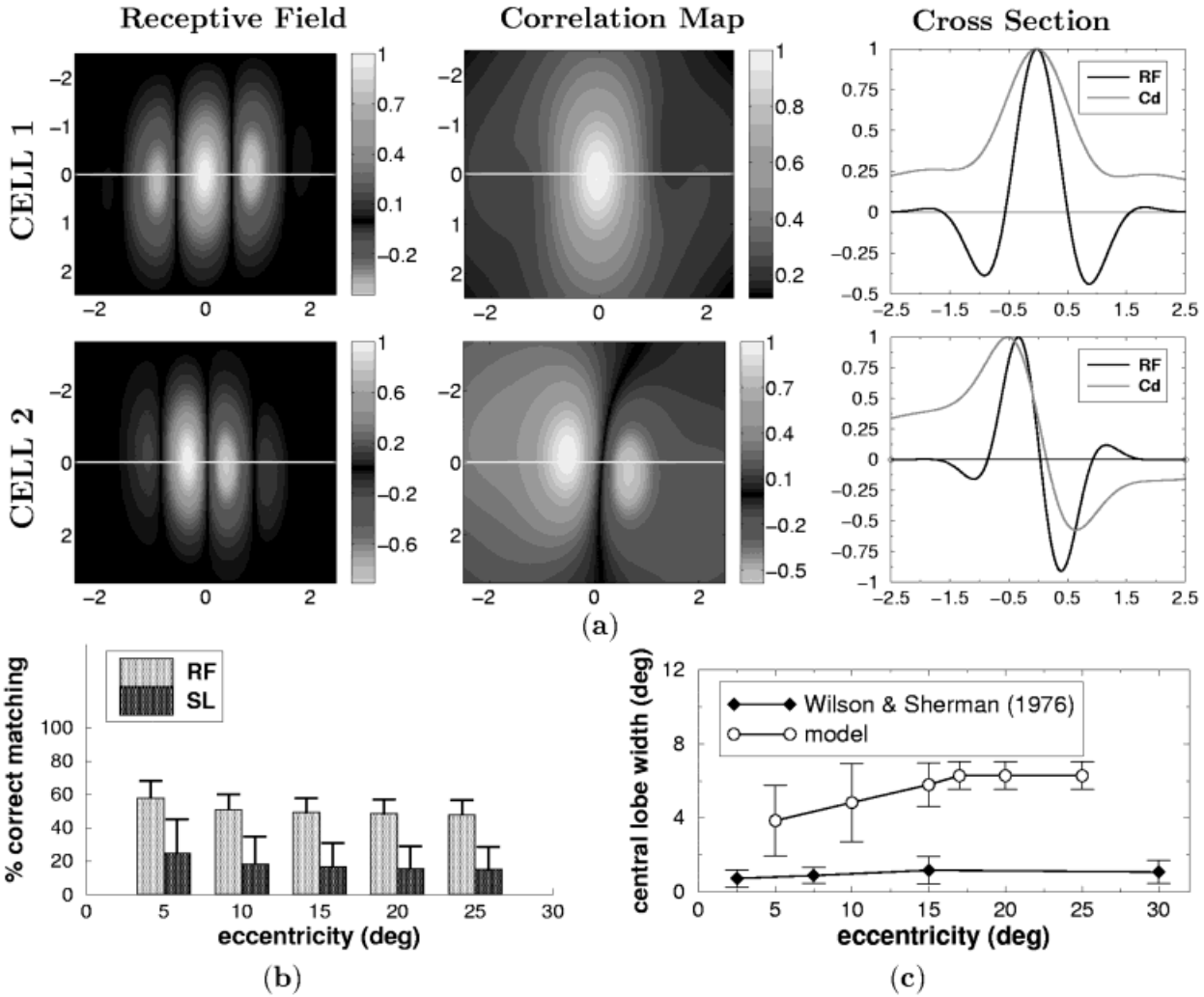

Fig. 2. Patterns of thalamocortical covarying activity measured when images of natural scenes were examined statically, that is, in the absence of eye movements. (*a*) The results for two simulated simple cells are shown on separate rows. For each of the two V1 units, the spatial receptive field (left panel), the measured correlation difference map (center panel), and a comparison between the receptive field and the correlation difference map along a cross section (right panel) are shown. Axis units are in degrees of visual angle. The horizontal lines on the left and center panels indicate the level at which the cross sections on the right panels were taken. (b) Matching percentages between correlation difference maps and the spatial structure of receptive-fields for all simulated simple cells. Each bar shows the average percentage of receptive field (RF, light bars) or receptive field side lobes (SL, dark bars) for which the correlation difference maps matched the sign of the subregions within the cortical receptive fields. Averages were evaluated over ten simulated simple cells. The results of simulations that replicated the characteristics of geniculate cells located at various angles of visual eccentricity are ordered along the *x* axis. (c) Comparison between the mean widths of the central lobe of cortical receptive fields measured by Wilson and Sherman (1976) in the cat (♦) and predicted by the patterns of covarying activity in the model (○) at various eccentricities.

by the correlation difference maps. Model data refer to cells in our modeling database with receptive fields composed of an odd number of subregions (5 out of 10 neurons). As shown by the curves in Fig. 2(c), the width of the central subregion predicted by the simulated patterns of covarying activity was substantially larger than the width measured in the cat at all the considered visual eccentricities.

The results of Fig. 2 are a direct consequence of the broad spatial correlations that characterize natural visual scenes. These correlations tend to drive synchronously geniculate cells with similar characteristics located at relatively large separations in the visual field. For comparison, Fig. 3 illustrates the situation before eye opening, when only spontaneous neural activity was present. The statistical structure of spontaneous activity was modeled on the basis of the correlated activity of retinal ganglion cells as measured by Mastronarde (1983) (see Methods). As shown by Figs. 3(a) and (b), in this case the measured patterns of covarying activity closely followed the spatial organization of simple cell receptive fields. The average matching percentage over the various angles of visual eccentricity was 94%. High matching percentages were also obtained in correspondence of the secondary subregions in cortical receptive fields, where the average matching was 90%. Thus, in the presence of spontaneous activity, ON-center and OFF-center geniculate cells covaried strongly with a cortical unit

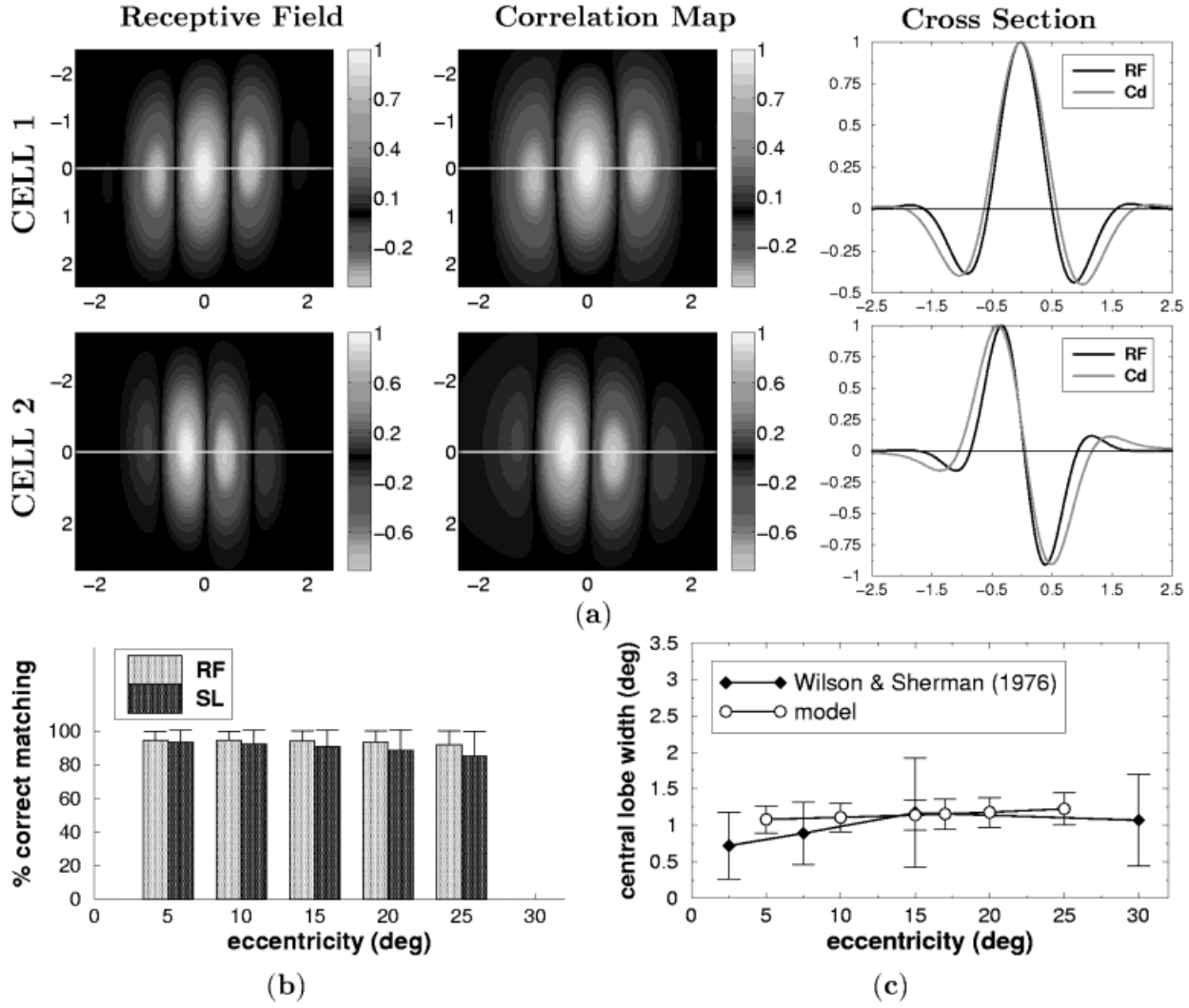

Fig. 3. Patterns of thalamocortical covarying activity in the presence of spontaneous neural activity. The layout of the panels and the graphic notations are the same as in Fig. 2.

only when their receptive fields overlapped, respectively, ON and OFF subregions in the cortical receptive field. Furthermore, as shown by Fig. 3(c), the width of the central lobe in cortical receptive fields predicted by the correlation difference maps was consistent with neurophysiological data at all angles of visual eccentricity.

The results of Figs. 2 and 3 indicate that while a Hebbian mechanism of synaptic plasticity is consistent with a segregation of geniculate afferents within the receptive fields of simple cells before eye opening, when narrow patterns of correlated activity exist in the retina, such a mechanism is not compatible with the structure of simple cell receptive fields during static presentation of natural visual input, when neural activity is influenced by the broad spatial correlations of natural scenes. In the simulations of Fig. 2, however, images of natural scenes were presented statically, and the input signals were not altered by the behavior of the observer as occurs during natural viewing conditions. To study the possible impact of eye movements on the structure of thalamocortical activity, we first simulated neural responses in two different experimental conditions: when eye movements included only large (non fixational) saccades, and during sustained visual fixation, that is, when only fixational eye movements were present.

Fig. 4 shows the results of simulations that replicated the characteristics of LGN units at 17 deg of visual eccentricity. In the presence of saccades only (top row of Fig. 4), patterns of covarying activity resembled those obtained with static presentation of natural images. On average, correlation difference maps matched the sign of cortical receptive fields in only 54% of the cases. Again, this mismatch was more pronounced in correspondence of the lateral subregions in the receptive fields of V1 units, where the average percentage of correct matching was only 22%. Fig. 4(d) illustrates the results obtained during sustained visual fixation. In this case, 120 fixation points were randomly selected for each image, and each fixation was maintained for a period of 4.6 s during which fixational eye movements occurred [see Fig. 4(c)]. As shown by the data in Fig. 4(d), during sustained visual fixation the patterns of thalamocortical connectivity predicted by the correlation difference maps were consistent with the organization of simple cell receptive fields. Correct matching occurred on average over 87% of the receptive fields and over 85% of the area covered by the lateral subregions.

Fig. 5 shows the results obtained in the more natural case in which images of natural scenes were scanned by unconstrained eye

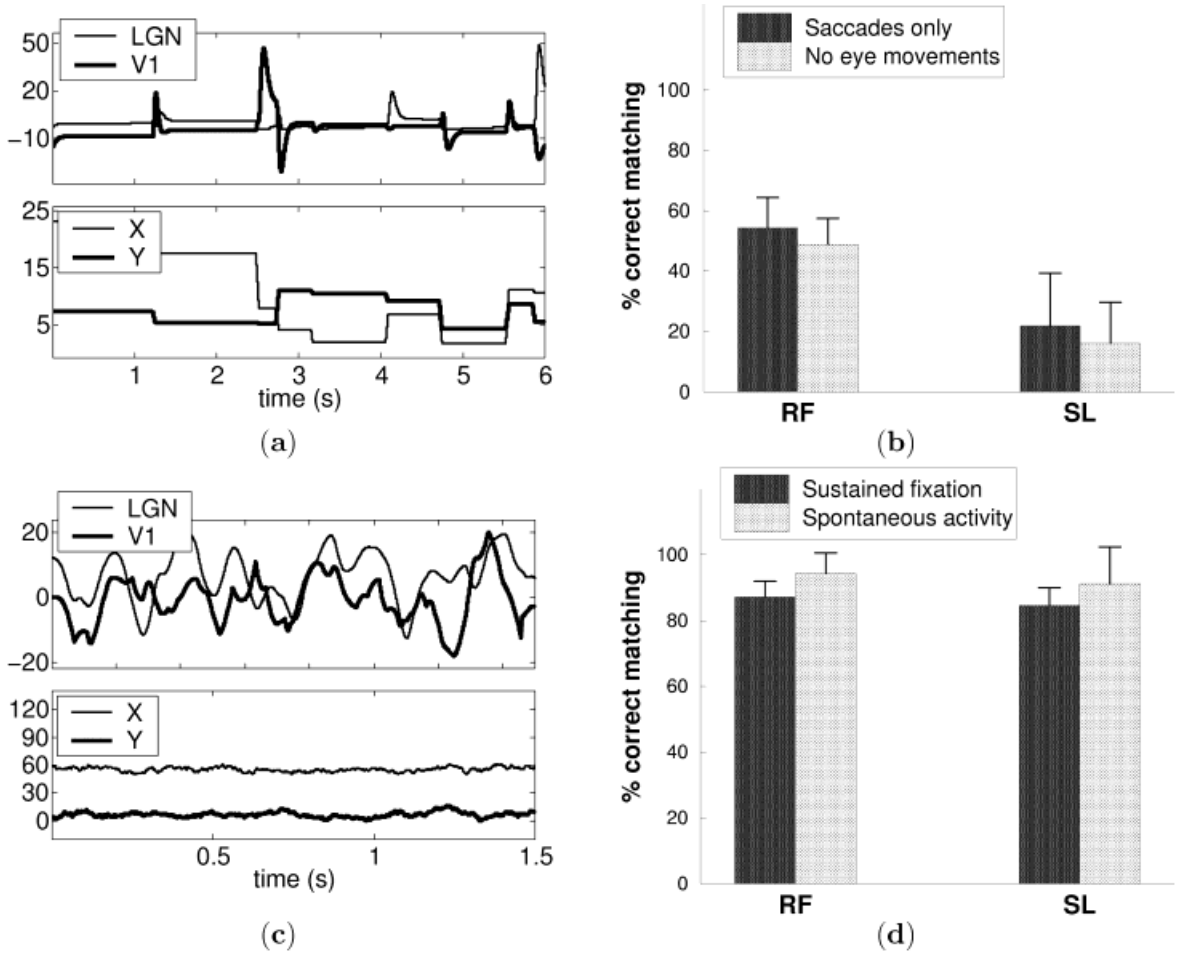

Fig. 4. Structure of thalamocortical covarying activity when images of natural scenes were scanned by specific types of eye movements. *Top row:* Case of saccades only. *Bottom Row:* Case of sustained visual fixation. (a) and (c) illustrate examples of simulated neural responses for a LGN neuron and a V1 simple cell (top graphs) during eye movements (bottom graphs). The *x* axis represents time. Units on the *y* axis of the eye movement graphs are in degrees in (a) and in minutes of arc in (c). The dark bars in (b) and (d) show the percentages of correct matching for the two types of eye movements. Matching percentages were evaluated both over the entire receptive-field area (RF) and in correspondence of the side lobes within the receptive fields (SL). The light bars are matching percentages for the cases of static presentation of natural visual input (in b) and spontaneous neural activity (in d), which are shown here for comparison.

movements. Sequences of eye movements included both large saccades and fixational instability. As shown in Fig. 5(b), which considers the case of 17 deg of visual eccentricity, when both large and small eye movements were simultaneously present, nonfixational saccades dominated the structure of covarying activity. Indeed, when levels of covariance were evaluated over the entire duration of a trial (6 s), correlation difference maps resembled those of Fig. 4(b) obtained with saccades only and did not match cortical receptive fields. In contrast, when the analysis was restricted to the periods of fixation in between saccades, the organization of receptive fields predicted by the correlation difference maps closely followed those of simulated simple cells. As illustrated by Fig. 5(c), high percentages of correct matching were obtained at all angles of visual eccentricity. In addition, the size of the larger subregion of receptive fields predicted by the patterns of covarying activity was in good agreement with neurophysiological measurements in the cat [Fig. 5(d)].

The results of Figs. 4 and 5 show that the broad spatial correlations of natural visual input have a reduced impact on correlation difference maps during the physiological instability of visual fixation. What are the factors responsible for this result?

An intuitive explanation can be given in terms of the influences of the spatial frequencies of the visual stimulus on neural activity during oculomotor behavior. In the presence of eye movements, the frequency content of the input signals to the retina depends both on the stimulus and the on relative motion between the stimulus and the eye. The degree by which different spatial-frequency bands affect correlation difference maps varies depending on the type of oculomotor activity. Fig. 6 shows the simulated activity of two ON-center LGN units (LGN A and B) and a simple cell (η) during a sequence of eye movements composed of two fixations separated by a saccade. As shown in the left panel of Fig. 6, the receptive fields of the two LGN units overlapped, respectively, an ON and an OFF subregion in the receptive field of the cortical cell. The three panels on the right side of Fig. 6 show the responses of the three units in the two cases of absence and presence of fixational eye movements. In the absence of fixational instability, cell responses settled on a steady value after the sac-

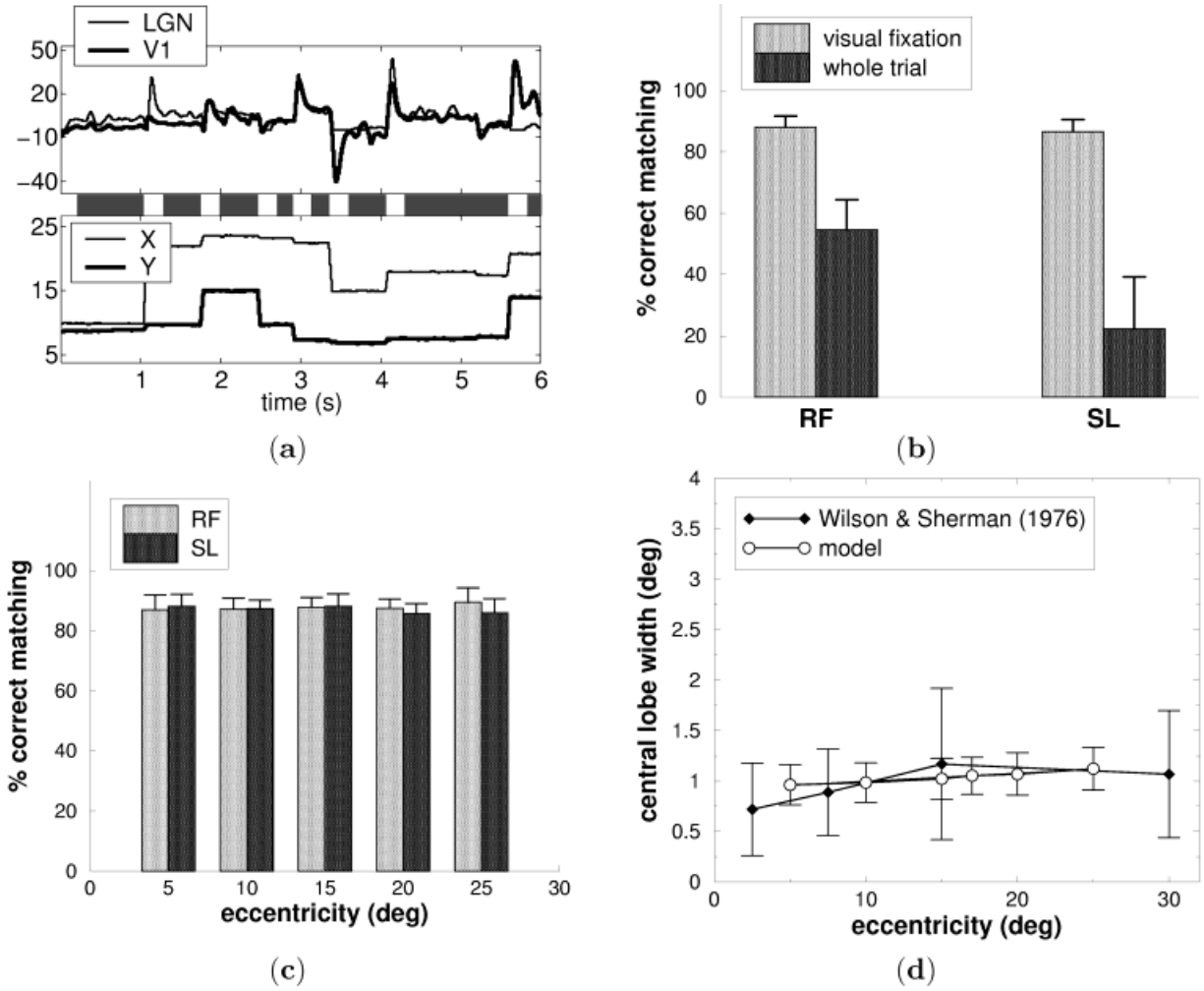

Fig. 5. Structure of thalamocortical covarying activity during free viewing of natural images. Simulated eye movements included both large saccades and small fixational eye movements. (a) Example of simulated responses for a geniculate and a cortical unit (*top*) during oculomotor behavior (*bottom*). The dark horizontal segments indicate the periods over which patterns of covarying activity were evaluated in the visual fixation case. (b) Percentages of correct matching between the receptive fields of V1 simple cells and the correlation difference maps at 17 deg of visual eccentricity. Levels of covariance were analyzed both over the entire duration of a trial (dark bars) and during the periods of visual fixation (light bars); both over the entire receptive-field area (RF) and in correspondence of the side lobes within the simple cell receptive fields (SL). (c) Matching percentages during visual fixation for various angles of visual eccentricity. Both the results obtained over the entire receptive field (RF) and over the side lobes (SL) are shown. (d) Comparison between the mean widths of the central lobe of cortical receptive fields measured by Wilson and Sherman (1976) (♦) and predicted by the patterns of covarying activity in the model (○) at various eccentricities.

cade. The cortical unit responded vigorously, as its receptive field landed on a suitable stimulus. Also the responses of the two geniculate units increased following the saccade, since their receptive fields moved from a dark region of the image to a brighter one. Thus, the responses of both LGN units covaried positively with the output of η ($\rho_{\eta A} = 0.91$ and $\rho_{\eta B} = 0.81$), despite the fact that the receptive fields of the two geniculate cells overlapped subregions of opposite polarity in η's receptive field. The origins of this result lie in the low spatial-frequency content of the scene. In a natural image, regions with different luminance like the dark and bright regions of Fig. 6 tend to be distant from each other and are therefore represented by low spatial-frequency harmonics. These low spatial frequencies, which are responsible for the broad spatial correlations that characterize images of natural scenes, appear as sustained components of geniculate responses during the periods of fixation. In the presence of large saccades, they strongly influence the levels of covariance between the responses of geniculate and cortical cells.

In the presence of fixational instability, the transient fluctuations in the input signals introduced by small eye movements modulate geniculate responses around their mean fixational values. In this case, each cell receives input from a small region surrounding its receptive field. Since low spatial-frequency components vary little over the small area covered by fixational instability, changes in the input signals are produced mainly by high-spatial-frequency harmonics, which determine how the scene changes locally. Thus, during the instability of visual fixation, low and high spatial frequencies appear respectively as sustained and dynamic components of geniculate responses. Correlation difference maps evaluated during the periods of fixation depend on the correlations

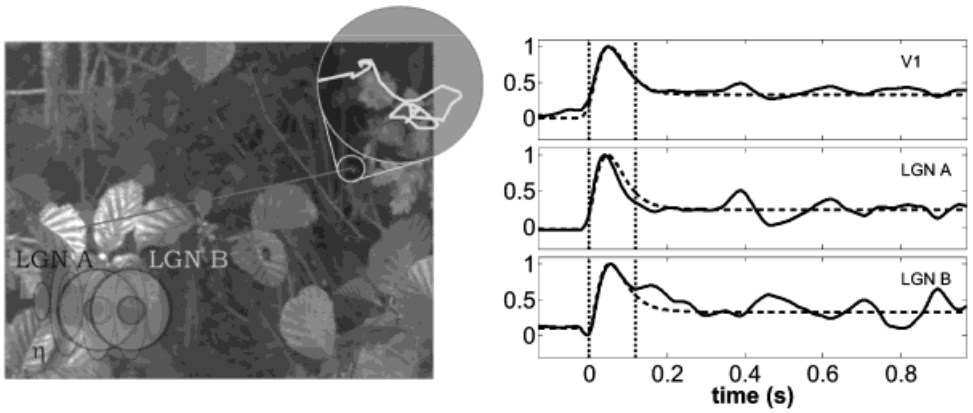

Fig. 6. Simulated responses of two ON-center geniculate cells and a V1 simple cell during a sequence of eye movements. (*Left*) The sequence consisted of two fixations separated by a saccade and is shown superimposed on the image. The enlarged insert shows the instability of visual fixation. The relative positions of cells receptive fields are shown in the bottom left corner. Geniculate units LGN *A* and *B* overlapped, respectively, an ON and an OFF region in the receptive field of the simple cell η. The distance between the receptive fields of the two geniculate units was 1.2 deg. (*Right*) Responses of the three simulated units. In each graph, the curves with continuous lines represent simulated responses in the case in which fixational instability occurred following the saccade. The dashed lines are simulated responses in the absence of fixational eye movements. The origin of the time axis is aligned with the onset of visual fixation. The two vertical lines mark the beginning of the intervals over which correlation coefficients were evaluated in the two cases described in the text. For both cases, the end of the interval coincided with the end of the trial. In the case of visual fixation, correlation coefficients were evaluated starting 120 ms after fixation onset to discount initial postsaccadic transients in neuronal responses.

between the dynamic components of cell responses, and are therefore heavily influenced by the high spatial frequencies of the stimulus. Due to the reduced impact of low spatial frequencies, correlation difference maps are little affected during fixation by the broad correlations of natural images. In the example of Fig. 6, after the saccade, the cortical unit η covaried positively with LGN A that overlapped an ON subregion in its receptive field ($\rho_{\eta A} = 0.93$) and negatively with LGN B that overlapped an OFF subregion ($\rho_{\eta B} = -0.46$).

This intuitive idea can be expressed more quantitatively by analyzing the contributions of different spatial-frequency bands to the correlated structure of the visual input during oculomotor activity. Fig. 7(a) compares the spatial correlation of the input to the retina, $I(x, y, t)$, to that of the same signal after high-pass filtering, $I_H(x, y, t)$. This second signal can be regarded as the main input contributor to the correlation difference maps evaluated during the periods of visual fixation. In Fig. 7(a), natural images were scanned by uniform motion at constant velocity. High-pass filtering was performed in the temporal domain by subtracting from the input at each spatial location its running average over an interval $T = 300$ ms (the average duration of visual fixation): $I_H(x, y, t) = I(x, y, t) - \bar{I}_T$. As illustrated by the power spectra in Fig. 7(a), high-pass filtered signals were less correlated with slow movements that, similar to the instability of visual fixation, covered less than 1 deg during the period of fixation. The different slopes of the curves obtained with different velocities indicate that, in principle, the visual system could control the degree of "whitening" of the input by selecting an appropriate oculomotor activity.

High-pass temporal filtering eliminates the slowly varying contributions originating from low spatial frequencies. The same result can be obtained by filtering directly in the spatial domain. Fig. 7(b) compares the power spectrum of a natural scene $S(x, y)$ to that of the high-pass filtered image $S_H(x, y)$ obtained by subtracting at each point (x, y) the average luminance evaluated over a local region W centered on (x, y): $S_H = S - \bar{S}_W$. The power spectra of both S and S_H were evaluated over the window W. Consistent with the scale-invariant structure of natural stimulation, the power spectrum of natural images was unaffected by the size of the window over which it was evaluated, as shown in the top graph of Fig. 7(b). However, this was not the case for the high-pass filtered images. Since removal of the spatial average eliminated scale invariance, S_H was less correlated in space (that is, its power spectrum was more flat) with smaller windows. As illustrated in the bottom graphs of Fig. 7(b), the power spectrum of this signal was substantially "whitened" when local means were evaluated over a window with size comparable to the extent of fixational instability.

It should be noted that the results of the previous simulations do not necessarily imply that the refinement and maintenance of cortical receptive fields require a learning rule based on the covariance of activity. Indeed, very similar results were obtained when levels of correlation (and not covariance) of thalamocortical activity were measured in simulations that included nonlinear elements of the responses of V1 units. It is known that for many V1 neurons the initial response to an unchanging stimulus tends to decline quickly, more rapidly than occurs in the responses of cells at earlier stages in the visual pathway. This decay is more rapid than what would be expected from the linear temporal transfer function (Tolhurst et al., 1980; Deangelis et al., 1993*b*; Chance et al., 1998; Müller et al., 1999). Whereas linear models predict that, after an initial transient, neuronal responses to a prolonged, steady flash should exhibit a well-maintained increase in activity, on the contrary the step responses of many simple and complex cells include only a small maintained response (Tolhurst et al., 1980; Deangelis et al., 1993*a*). This fast decay of V1 cells is likely to play an important role during natural viewing conditions, when natural scenes are scanned by sequences of eye movements. Following a saccade, the stimulus in the receptive field of a V1 cell changes little during the brief periods of visual fixation. A nonlinear decay to unchanging stimuli is likely to attenuate cell responses

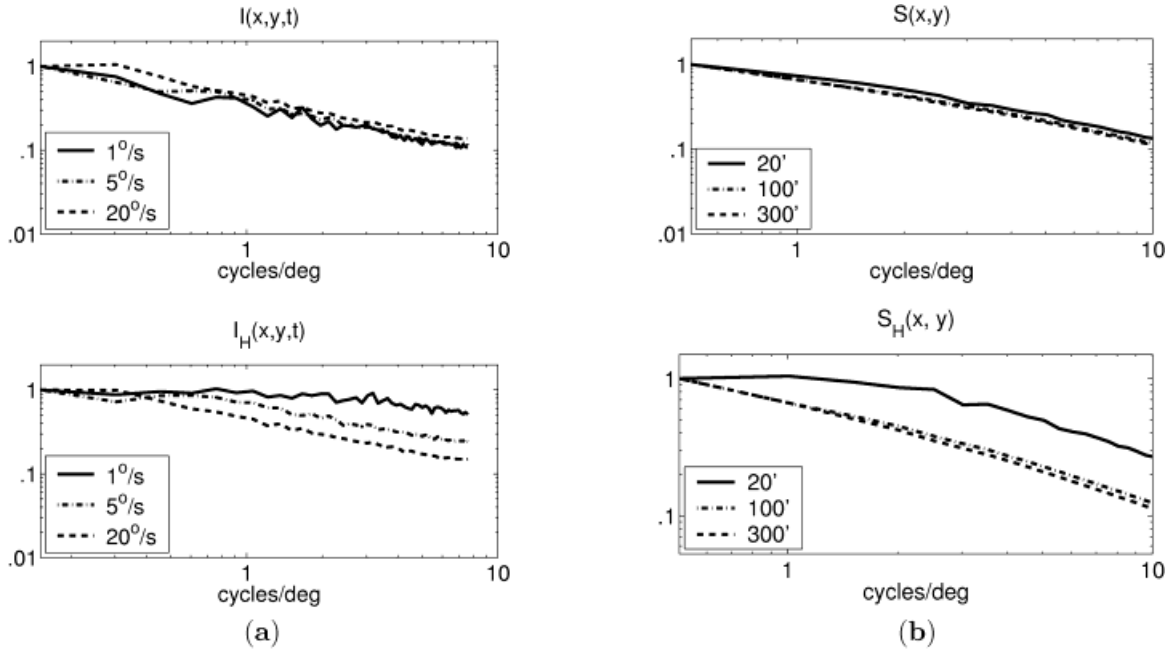

Fig. 7. Correlated structure of the input signals to the retina during active scanning of images of natural scenes. (a) Comparison between the power spectrum of the input to the retina during oculomotor activity, $I(x, y, t)$ (*top*), and that of the same signal after removal of its running average $I_H(x, y, t) = I(x, y, t) - \bar{I}_T$ (*bottom*). T was 300 ms. Natural images were scanned by uniform drift at constant velocity. The results for three velocities (1 deg/s, 5 deg/s, 20 deg/s) are shown. (b) Comparison between the power spectrum of natural visual input before (*top*) and after high-pass filtering (*bottom*). High-pass filtering was implemented by subtracting at each point of the image $S(x, y)$ its local mean over a window W: $S_H = S - \bar{S}_W$. Power spectra were evaluated over W. The data are average values of the power spectrum obtained over all the images included in the database. The results for three different amplitudes of W (20′, 100′ and 300′) are shown. In every panel, the x axis represents spatial frequency, and power spectra are normalized to provide clear comparisons.

to the sustained component of the visual input, thus emphasizing responses to the dynamic component introduced by fixational instability.

Fig. 8 shows the result of simulations in which the model was extended to introduce a nonlinear term that replicated the fast decay of V1 neurons to steady stimuli (see Methods). As illustrated in Fig. 8(a), this nonlinear module attenuated the simulated response to a step stimulus, while preserving responses to dynamic inputs. Figs. 8(b–d) show the results obtained in the case in which images of natural scenes were scanned by unconstrained eye movements that included both large saccades and fixational instability. In this case, levels of correlation were evaluated both over the entire duration of a trial and during the periods of fixation in between saccades. Patterns of correlation measured during fixation closely followed those of simulated simple cells. As illustrated by Fig. 8(c), high percentages of correct matching were obtained at all angles of visual eccentricity, and the size of the larger subregion of receptive fields predicted by the levels of correlation was in good agreement with neurophysiological measurements in the cat [Fig. 8(d)].

Fig. 9 summarizes the results of our simulations with nonlinear cortical responses. In these simulations, the small spatial scale of fixational eye movements and the fast adaptation of simulated cortical units operated jointly to decorrelate neural activity. As illustrated in Fig. 9, levels of correlation did not match cortical receptive fields in simulations in which the spatial scale of fixational eye movements was amplified or when nonlinear adaptation was eliminated. These results contrast with the case of white noise input, in which patterns of correlation followed closely the structure of simple cell receptive fields even in the absence of oculomotor activity and the nonlinear adaptation of V1 units (black bars in Fig. 9). In the presence of natural visual stimulation, the interaction between small fixational eye movements (which introduced spatially decorrelated fluctuations in the input signals) and nonlinear cortical adaptation (which attenuated the responses to the slowly varying, spatially correlated component of natural input) enabled the establishment of a regime of thalamocortical activity with second-order statistics similar to that observed in the presence of white noise. This pattern of correlated activity is consistent with a refinement of cortical receptive fields.

Discussion

Many features of the responses of V1 neurons develop before eye opening and are further refined by visual experience. How can the same mechanism of synaptic plasticity account for both the initial maturation of neuronal selectivity and its later refinement in the presence of neural activity with such different statistical structure as endogenous spontaneous activity and visually driven responses? After eye opening, the sampling of sensory information depends on the way an organism moves within the environment. By constraining input sensory signals, motor behavior may alter the statistical structure of neural activity and influence the refinement of perceptual systems during early sensory experience. By showing that the spatiotemporal structure of neural activity during visual fixation is compatible with the organization of the receptive

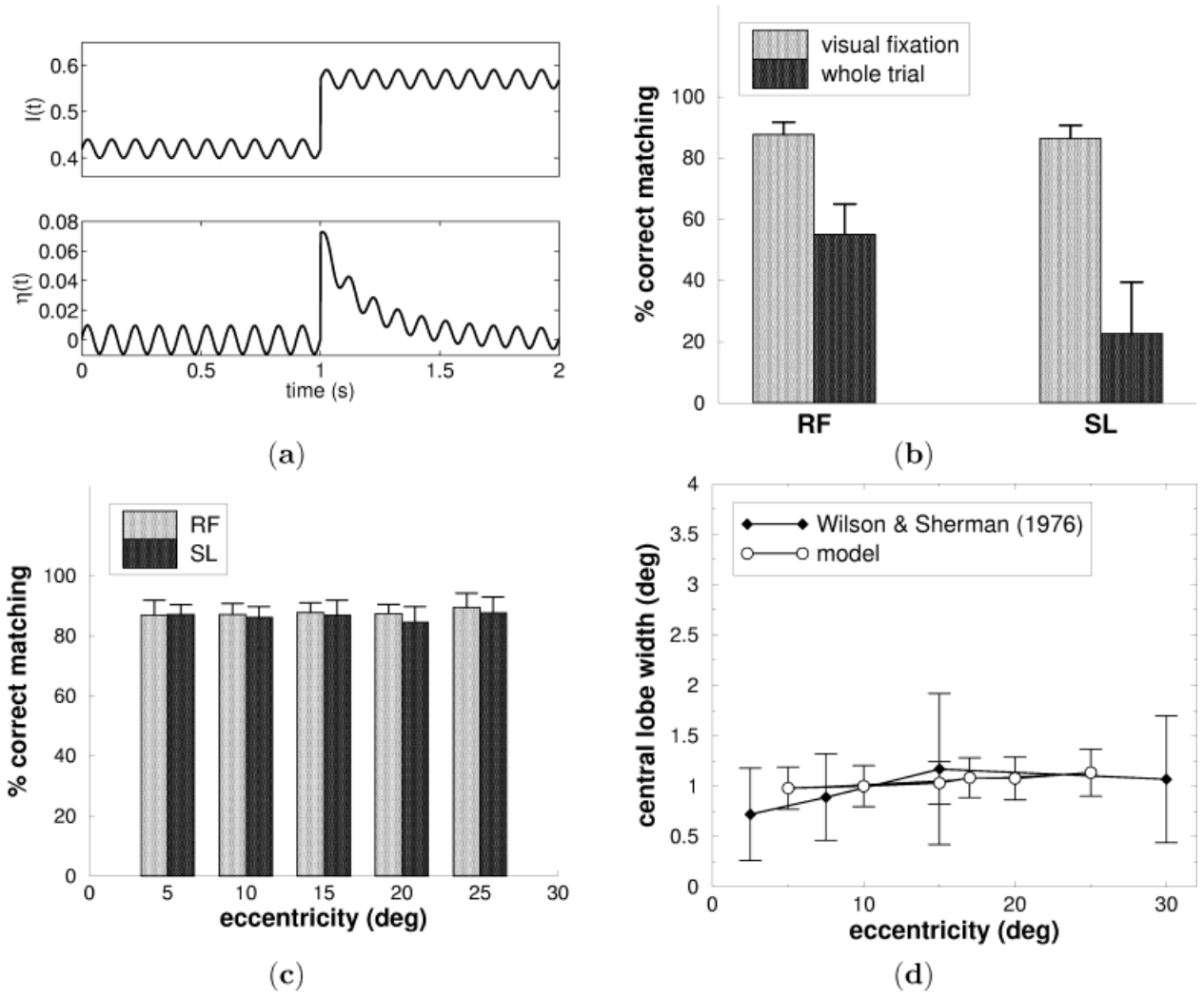

Fig. 8. Structure of thalamocortical correlated activity during free viewing of natural images. Levels of correlation were evaluated when the model included a nonlinear component that replicated the fast decay of V1 units to unchanging stimuli. (a) Response of the nonlinear element of the model to an input current composed of the superposition of a step function and a 10-Hz sinusoidal modulation. After a transitory period, the model responds only to the dynamic component of the input. (b) Percentages of correct matching between the receptive fields of V1 simple cells and patterns of correlated activity at 17 deg of visual eccentricity. Levels of correlation were analyzed both over the entire duration of a trial (dark bars) and during the periods of visual fixation (light bars); both over the entire receptive-field area (RF) and in correspondence of the side lobes within the simple cell receptive fields (SL). (c) Matching percentages during visual fixation for various angles of visual eccentricity. Both the results obtained over the entire receptive field (RF) and over the side lobes (SL) are shown. (d) Comparison between the mean widths of the central lobe of cortical receptive fields measured by Wilson and Sherman (1976) (♦) and predicted by the patterns of correlated activity in the model (○) at various eccentricities.

fields of simple cells, the present study supports the hypothesis that the refinement and maintenance of orientation selectivity after eye opening could be mediated by the same Hebbian process of synaptic plasticity that has been proposed to be responsible for the initial emergence of a segregation of thalamic afferents to the cortex (Linsker, 1986; Miyashita & Tanaka, 1992; Miller, 1994).

In the model, three elements determined the structure of neural activity: the statistical properties of the visual input, the response characteristics of simulated neurons, and the way visual information was sampled by means of oculomotor behavior. In the absence of eye movements, when only the first two elements contributed, the patterns of thalamocortical activity were heavily influenced by the broad spatial correlations of natural images. These input correlations synchronously activated wide pools of ON- or OFF-center cells in the LGN, which covaried strongly with simulated V1 neurons, a pattern of activity that is not compatible with a Hebbian segregation of geniculate afferents within simple cell receptive fields. On the contrary, in simulations that modeled the oculomotor behavior of the cat, fixational eye movements introduced spatially decorrelated fluctuations in the input signals. Both simulated LGN and V1 cell responses were modulated by these spatiotemporal changes in the visual input. Thus, during visual fixation, levels of covariance between geniculate and cortical responses (and also levels of correlation when the nonlinear adaptation of V1 units was taken into account) were constrained by the structure of the receptive fields of V1 and LGN neurons similar to before eye opening.

In a previous modeling study, the patterns of covariance of geniculate activity during the small eye movements of visual

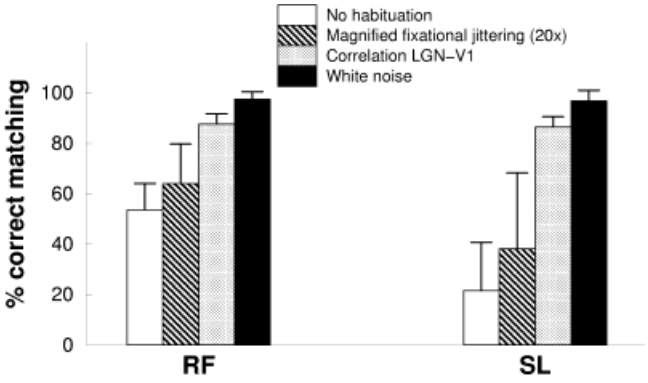

Fig. 9. Matching between the receptive fields of V1 simple cells and the levels of correlation in thalamocortical activity measured under various experimental conditions. Matching percentages were evaluated both over the entire receptive field (RF) and in correspondence of the secondary subregions of cortical receptive fields (SL). Matching percentages obtained at 17 deg of visual eccentricity with normal fixational instability and nonlinear adaptation of V1 responses (*gray bar*) are compared to those obtained in the following conditions: (*white bar*) absence of cortical adaptation. Modeled cortical units did not include the nonlinear component. (*striped bar*) Amplified fixational instability. The window of fixational jittering was magnified by a factor of 20. (*black bar*) Case of decorrelated input. White noise was presented to the model in the absence of both fixational instability and cortical adaptation.

fixation were found to match the average structure of the receptive fields of simple cells at various angles of visual eccentricity (Rucci et al., 2000). By simultaneously and independently simulating the activity of both geniculate and V1 simple cells during oculomotor behavior, the results of this study extend our previous work in several important ways. First, they show that fixational fluctuations in the input signals are very effective in driving models of cortical cells and in shaping the correlated structure of thalamocortical activity. According to our model, the process of maintenance and refinement of cortical receptive fields would be sensitive to the synchronous modulations of thalamic responses that originate from fixational eye movements. Second, this study clarifies the mechanisms by which, during visual fixation, the broad correlations of natural visual input may loose their influence on the statistical structure of neural activity. During visual fixation, the jittering of the eye enhances neuronal responses to high spatial-frequency signals, which contribute little to the correlated structure of natural scenes. Third, it shows that in addition to a general consistency between thalamic activity and the average organization of simple cell receptive fields, levels of correlation/covariance of thalamocortical activity are compatible with the specific structure of the receptive fields of individual V1 neurons. Since during visual fixation the second-order statistics of neural activity resemble that present before eye opening, cells with very different receptive fields will continue their refinement of orientation selectivity.

Small fixational eye movements are a common feature of the oculomotor behavior of different species. In humans, several types of fixational eye movements have been observed, including small saccades with amplitudes in the range 2–30 arcmin, slow drifts with speed less than 20 arcmin/s, and physiological nystagmus, a high-frequency tremor with amplitude smaller than 1 arcmin (Ditchburn, 1973; Steinman et al., 1973). In addition to humans, fixational eye movements have been observed in the monkey (Skavenski et al., 1975), the cat (Pritchard & Heron, 1960), the rabbit (Collewijn & Van Der Mark, 1972), the turtle (Greschner et al., 2002), and even the owl (Steinbach & Money, 1973), a species whose eyes are often considered immobile. Although it has long been known that stabilized images (i.e. images that move synchronously with the eye) tend to fade from visual awareness, it is not clear whether fixational eye movements play a functionally meaningful role in visual processes beyond simply refreshing neural activity.

Neuronal responses to the input changes produced by fixational eye movements have also been observed. Indeed, it has been suggested that the instability of visual fixation may contribute to the high variability of cortical responses measured in awake monkeys (Gur & Snodderly, 1987). In the macaque, fixational eye movements strongly modulate the responses of neurons in different cortical areas (Gur et al., 1997; Leopold & Logothetis, 1998; Martinez-Conde et al., 2000), and neurons in the primary visual cortex can be sorted in different populations based on their responses to the two main components of fixational eye movements, saccades and drifts (Snodderly et al., 2001). In the cat, similar investigations on the influence of fixational eye movements on neural activity have not been performed. Nevertheless, saccades as small as 0.5 deg, which are likely to affect neural responses, occur frequently in the cat (Winterson & Robinson, 1975). In addition, the velocity of cat's postsaccadic drift has been measured around 10–15 deg/s (Olivier et al., 1993), a speed that is likely to activate cortical cells.

It is important to notice that the main effect of fixational instability in our simulations, that is the introduction of a spatially decorrelated component in the input signals that, during visual fixation, is effective in driving cell responses is a robust phenomenon that does not depend on the precise characteristics of the model. While simulated eye movements were designed to replicate the oculomotor behavior of the cat, any type of fixational jittering, regardless of its sources, would have a similar impact on the statistical structure of neural activity, as long as it occurs within a relatively small spatial window. Thus, the results of this paper are little affected by possible inaccuracies in the simulations of cat eye movements and can be directly extended to free-viewing conditions in which eye movements may combine with small movements of the head and the body to give rise to greater fixational instability. Results were also little affected by the way the nonlinear features of cell responses were modeled. Virtually identical results were obtained when rectification in the LGN was absent or when it was increased to eliminate half of the range of possible response values. In the simulations that included the nonlinear adaptation of V1 units, the adaptive RC circuit was preferred over other methods that model the fast adaptation of cortical cells (Abbott et al., 1997; Tsodyks & Markram, 1997; Okatan & Grossberg, 2000) because it operated directly on the mean instantaneous firing rate, a more convenient signal to use than the raw train of spikes in simulations that involve massive statistical averaging such as the ones described in this paper. However, any mechanism that quickly attenuates the sensitivity to stationary stimuli would have a similar decorrelating effect during visual fixation. Indeed, once the influence of the broad input correlations introduced by low spatial-frequency harmonics is attenuated, the structure of correlated activity is primarily determined by the spatial organization of cell receptive fields. The spatial characteristics of the receptive fields of geniculate and V1 simple cells are among the most investigated features of neurons in the visual system, and the kernels of our models were direct implementations of neurophysiological measurements.

While sources of fixational instability other than eye movements exist during natural viewing, a consequence of this study is that visual conditions that disrupt normal oculomotor activity may impair the development of the response characteristics of V1 simple cells. Consistent with this prediction, an impairment in the plasticity underlying orientation selectivity has been observed in kittens exposed to visual experience with their eyes paralyzed. Whereas a few hours of normal visual experience within a critical period are sufficient to reestablish orientation-selective responsesin dark-reared kittens, elimination of eye movements during light exposure prevents such restoration (Buisseret et al., 1978; Gary-Bobo et al., 1986). In the presence of eye movements, a normal reestablishment of orientation selectivity occurs even if other movements of the body are selectively prevented (Buisseret & Gary-Bobo, 1979). Furthermore, a reduction in the percentage of orientation-selective cells has also been reported in cats raised under low-frequency stroboscopic light (Cynader et al., 1973), a well-investigated illumination condition that eliminates fixational instability. The abnormal increase in the size of simple-cell receptive fields observed in these kittens is consistent with the patterns of correlated activity measured in our simulations that did not include fixational eye movements. Interestingly, orientation selectivity appears normal in cats reared under high frequency (8 Hz) of stroboscopic light (Cynader & Chernenko, 1976), when the presence of several flashes within a single fixation may reestablish the effect of fixational jittering.

While the focus of this study has been on visual development, it should be observed that a decorrelation of neuronal responses during visual fixation might also have important functional implications. It is a long-standing proposal that one of the goals of the early stages of the visual system is to eliminate the statistical redundancy of input signals in order to achieve more compact and efficient representations (Barlow, 1961). Consistent with this proposal, it has been observed that geniculate and retinal ganglion cells may attenuate spatial and temporal correlations of the input signals (Atick & Redlich, 1992). The results of our simulations suggest that fixational eye movements may contribute by further decorrelating component of the input signals that are effective in driving cortical responses. Further theoretical and experimental studies are necessary to investigate this hypothesis and better characterize the impact of fixational instability on neuronal responses.

Acknowledgment

This material is based upon work supported by the National Science Foundation under Grant No. EIA-0130851.

References

Abbott, L.F., Varela, J.A., Sen, K. & Nelson, S.B. (1997). Synaptic depression and cortical gain control. *Science* **275**, 220–224.

Albus, K. & Wolf, K. (1984). Early postnatal development of neuronal function in the kitten's visual cortex: A laminar analysis. *Journal of Physiology* **348**, 153–185.

Atick, J.J. & Redlich, A.N. (1992). What does the retina knows about natural scenes. *Neural Computation* **4**, 196–210.

Barlow, H.B. (1961). Possible principles underlying the transformation of sensory messages. In *Sensory Communication*, ed. Rosenblith W.A., Pp. 217–234. Cambridge, Massachusetts: MIT Press.

Bendat, J.S. & Piersol, A.G. (1986). *Random Data: Analysis and Measurement Procedures*. New York: John Wiley & Sons Inc.

Blakemore, C. & Van Sluyters, R.C. (1975). Innate and environmental factors in the development of the kitten's visual cortex. *Journal of Physiology* **248**, 663–716.

Buisseret, P. (1995). Influence of extraocular muscle proprioception on vision. *Physiological Reviews* **75**, 323–338.

Buisseret, P. & Gary-Bobo, E. (1979). Development of visual cortical orientation specificity after dark-rearing: Role of extraocular proprioception. *Neuroscience Letters* **13**, 259–263.

Buisseret, P., Gary-Bobo, E. & Imbert, M. (1978). Ocular motility and recovery of orientational properties of visual cortical neurons in dark-reared kittens. *Nature* **272**, 816–817.

Buisseret, P. & Imbert, M. (1976). Visual cortical cells: Their developmental properties in normal and dark-reared kittens. *Journal of Physiology* **255**, 511–525.

Cai, D., DeAngelis, G.C. & Freeman, R.D. (1997). Spatiotemporal receptive field organization in the lateral geniculate nucleus of cats and kitten. *Journal of Neurophysiology* **78**, 1045–1061.

Chance, F.S., Nelson, S.B. & Abbott, L.F. (1998). Synaptic depression and the temporal response characteristics of V1 cells. *Journal of Neuroscience* **18**, 4785–4799.

Changeux, J.P. & Danchin, A. (1976). Selective stabilization of developing synapses as a mechanism for the specification of neuronal networks. *Nature* **264**, 705–712.

Chapman, B. & Stryker, M.P. (1993). Development of orientation selectivity in ferret visual cortex and effects of deprivation. *Journal of Neuroscience* **13**, 5251–5262.

Chapman, B., Zahs, K.R. & Stryker, M.P. (1991). Relation of cortical cell orientation selectivity to alignment of receptive fields of the geniculocortical afferents that arborize within a single orientation column in ferret visual cortex. *Journal of Neuroscience* **11**, 1347–1358.

Chung, S. & Ferster, D. (1998). Strength and orientation tuning of the thalamic input to simple cells revealed by electrically evoked cortical suppression. *Neuron* **20**, 1177–1189.

Collewijn, H. & Van Der Mark, F. (1972). Ocular stability in variable feedback conditions in the rabbit. *Vision Research* **36**, 47–57.

Crair, M.C., Gillespie, D.C. & Stryker, M.P. (1998). The role of visual experience in the development of columns in cat visual cortex. *Science* **279**, 566–570.

Cynader, M., Berman, N. & Hein, A. (1973). Cats reared in stroboscopic illumination: Effects on receptive fields in visual cortex. *Proceedings of the National Academy of Sciences of the U.S.A.* **70**, 1353–1354.

Cynader, M. & Chernenko, G. (1976). Abolition of direction selectivity in the visual cortex of the cat. *Science* **193**, 504–505.

DeAngelis, G.C., Ohzawa, I. & Freeman, R.D. (1993*a*). Spatiotemporal organization of simple-cell receptive fields in the cat's striate cortex. I. General characteristics and postnatal development. *Journal of Neurophysiology* **69**, 1091–1117.

DeAngelis, G.C., Ohzawa, I. & Freeman, R.D. (1993*b*). Spatiotemporal organization of simple-cell receptive fields in the cat's striate cortex. II. Linearity of temporal and spatial summation. *Journal of Neurophysiology* **69**, 1118–1135.

DeValois, R.L. & DeValois, K.K. (1990). *Spatial Vision*. New York: Oxford University Press.

Ditchburn, R. (1973). *Eye Movements in Relation to Retinal Action*. Oxford: Clarendon Press.

Ferster, D., Chung, S. & Wheat, H. (1996). Orientation selectivity of thalamic input to simple cells of cat visual cortex. *Nature* **380**, 249–252.

Field, D.J. (1987). Relations between the statistics of natural images and the response properties of cortical cells. *Journal of the Optical Society of America A* **4**, 2379–2394.

Freeman, R.D. & Bonds, A.B. (1979). Cortical plasticity in monocularly deprived immobilized kittens depends on eye movement. *Science* **206**, 1093–1095.

Fregnac, Y. & Imbert, M. (1978). Early development of visual cortical cells in normal and dark-reared kittens: Relationship between orientation selectivity and ocular dominance. *Journal of Physiology* **278**, 27–44.

Fregnac, Y., Shulz, D., Thorpe, S. & Bienenstock, E. (1992). Cellular analogs of visual cortical epigenesis. I. Plasticity of orientation selectivity. *Journal of Neuroscience* **12**, 1280–1300.

Gary-Bobo, E., Milleret, C. & Buisseret, P. (1986). Role of eye movements in developmental process of orientation selectivity in the kitten visual cortex. *Vision Research* **26**, 557–567.

Greschner, M., Bongard, M., Rujan, P. & Ammermüller, J. (2002). Retina ganglion cell synchronization by fixational eye movements improves feature estimation. *Nature* **5**, 341–347.

Gur, M., Beylin, A. & Snodderly, D.M. (1997). Response variability of neurons in primary visual cortex (V1) of alert monkeys. *Journal of Neuroscience* **17**, 2914–2920.

Gur, M. & Snodderly, D.M. (1987). Studying striate cortex neurons in behaving monkeys: Benefits of image stabilization. *Vision Research* **27**, 2081–2087.

Hirsch, H. & Spinelli, D. (1970). Visual experience modifies distribution of horizontally and vertically oriented receptive fields in cats. *Science* **168**, 869–871.

Hirsch, H.V.B. (1985). The role of visual experience in the development of cat striate cortex. *Cellular and Molecular Neurobiology* **5**, 103–121.

Hubel, D.H. & Wiesel, T.N. (1962). Receptive fields, binocular interaction and functional architecture in the cat's visual cortex. *Journal of Physiology* **160**, 106–154.

Ikeda, H. & Wright, M.J. (1975). The relationship between the 'sustained-transient' and the 'simple-complex' classifications of neurones in area 17 of the cat. *Journal of Physiology* **244**, 58P–59P.

Jones, J.P. & Palmer, L.A. (1987*a*). An evaluation of the two-dimensional gabor filter model of simple receptive fields in cat striate cortex. *Journal of Neurophysiology* **58**, 1233–1258.

Jones, J.P. & Palmer, L.A. (1987*b*). The two-dimensional spatial structure of simple receptive fields in cat striate cortex. *Journal of Neurophysiology* **58**, 1187–1211.

Lee, D. & Malpeli, J.G. (1998). Effect of saccades on the activity of neurons in the cat lateral geniculate nucleus. *Journal of Neurophysiology* **79**, 922–936.

Leopold, D.A. & Logothetis, N.K. (1998). Microsaccades differentially modulate neural activity in the striate and extrastriate visual cortex. *Experimental Brain Research* **123**, 341–345.

Linsenmeier, R.A., Frishman, L.J., Jakiela, H.G. & Enroth-Cugell, C. (1982). Receptive field properties of X and Y cells in the cat retina derived from contrast sensitivity measurements. *Vision Research* **22**, 1173–1183.

Linsker, R. (1986). From basic network principles to neural architecture: Emergence of orientation-selective cells. *Proceedings of the National Academy of Sciences of the U.S.A.* **83**, 8390–8394.

Martinez-Conde, S., Macknik, S. & Hubel, D.H. (2000). Microsaccadic eye movements and firing of single cells in the striate cortex of macaque monkeys. *Nature Neuroscience* **3**, 251–258.

Mastronarde, D.N. (1983). Correlated firing of cat retinal ganglion cells. I. Spontaneously active inputs to X and Y cells. *Journal of Neurophysiology* **49**, 303–323.

Miller, K.D. (1994). A model of the development of simple cell receptive fields and the ordered arrangement of orientation columns through activity-dependent competition between ON- and OFF- center inputs. *Journal of Neuroscience* **14**, 409–441.

Miller, K.D., Erwin, E. & Kayser, A. (1999). Is the development of orientation selectivity instructed by activity? *Journal of Neurobiology* **41**, 44–57.

Miyashita, M. & Tanaka, S. (1992). A mathematical model for the self-organization of orientation columns in visual cortex. *Neuroreport* **3**, 69–72.

Müller, J.R., Metha, A.B., Krauskopf, J. & Lennie, P. (1999). Rapid adaptation in visual cortex to the structure of images. *Science* **285**, 1405–1408.

Okatan, M. & Grossberg, S. (2000). Frequency-dependent synaptic potentiation, depression and spike timing induced by Hebbian pairing in cortical pyramidal neurons. *Neural Networks* **13**, 699–708.

Olivier, E., Grantyn, A., Chat, M. & Berthoz, A. (1993). The control of slow orienting eye movements by tectoreticulospinal neurons in the cat: Behavior, discharge patterns and underlying connections. *Experimental Brain Research* **93**, 435–449.

Pettigrew, J.D. (1974). The effect of visual experience on the development of stimulus specificity by kitten cortical neurons. *Journal of Physiology* **237**, 49–74.

Pritchard, R.M. & Heron, W. (1960). Small eye movements of the cat. *Canadian Journal of Psychology* **14**, 131–137.

Reid, R.C. & Alonso, J.M. (1995). Specificity of monosynaptic connections from thalamus to visual cortex. *Nature* **378**, 281–284.

Rucci, M., Edelman, G.M. & Wray, J. (2000). Modeling LGN responses during free-viewing: A possible role of microscopic eye movements in the refinement of cortical orientation selectivity. *Journal of Neuroscience* **20**, 4708–4720.

Ruderman, D.L. & Bialek, W. (1994). Statistics of natural images: Scaling in the woods. *Physics Review Letters* **73**, 814–817.

Sengpiel, F., Stawinski, P. & Bonhoeffer, T. (1999). Influence of experience on orientation maps in cat visual cortex. *Nature Neuroscience* **2**, 727–732.

Sherk, H. & Stryker, M. (1976). Quantitative study of cortical orientation selectivity in visually inexperienced kitten. *Journal of Neurophysiology* **39**, 63–70.

Singer, W. & Raushecker, J. (1982). Central-core control of developmental plasticity in the kitten visual cortex II. Electrical activation of mesencephalic and diencephalic projections. *Experimental Brain Research* **47**, 22–233.

Skavenski, A., Robinson, D., Steinman, R. & Timberlake, G. (1975). Miniature eye movements of fixation in rhesus monkey. *Vision Research* **15**, 1269–1273.

Snodderly, D.M., Kagan, I. & Gur, M. (2001). Selective activation of visual cortex neurons by fixational eye movements: Implications for neural coding. *Visual Neuroscience* **18**, 259–277.

Steinbach, M.J. & Money, K.E. (1973). Eye movements of the owl. *Vision Research* **13**, 889–891.

Steinman, R.M., Haddad, G.M., Skavenski, A.A. & Wyman, D. (1973). Miniature eye movement. *Science* **181**, 810–819.

Stent, G.S. (1973). A physiological mechanism for Hebb's postulate of learning. *Proceedings of the National Academy of Sciences of the U.S.A.* **70**, 997–1001.

Stryker, M.P. & Harris, W.A. (1986). Binocular impulse blocakade prevents formation of ocular dominance columns in the cat's visual cortex. *Journal of Neuroscience* **6**, 2117–2133.

Stryker, M.P., Sherk, H., Leventhal, A.G. & Hirsch, H.V.B. (1978). Physiological consequences for the cat's visual cortex of effectively restricting early visual experience with oriented contours. *Journal of Neurophysiology* **41**, 896–909.

Tolhurst, D.J., Walker, N.S., Thompson, I.D. & Dean, A.F. (1980). Non-linearities of temporal summation in neurones in area 17 of the cat. *Experimental Brain Research* **38**, 431–435.

Tsodyks, M.V. & Markram, H. (1997). The neural code between neocortical pyramidal neurons depends on neurotransmitter release probability. *Proceedings of the National Academy of Sciences of the U.S.A.* **94**, 719–723.

Tsodyks, M.V., Pawelzik, K. & Markram, H. (1998). Neural networks with dynamic synapses. *Neural Comp* **10**, 821–835.

van Hateren, J.H. & van der Schaaf, A. (1998). Independent component filters of natural images compared with simple cells in primary visual cortex. *Proceedings of the Royal Society B* (London) **265**, 359–366.

Varela, J., Sen, K., Gibson, J., Fost, J., Abbott, L.F. & Nelson, S.B. (1997). A quantitative description of short-term plasticity at excitatory synapses in layer 2/3 of rat primary visual cortex. *Journal of Neuroscience* **17**, 7926–7940.

Weliki, M. & Katz, L.C. (1997). Disruption of orientation tuning in visual cortex by artificially correlated neuronal activity. *Nature* **386**, 680–685.

White, L.E., Coppola, D.M. & Fitzpatrick, D. (2001). The contribution of sensory experience to the maturation of orientation selectivity in ferret visual cortex. *Nature* **411**, 1049–1052.

Wilson, J.R. & Sherman, S.M. (1976). Receptive-field characteristics of neurons in the cat striate cortex: Changes with visual field eccentricity. *Journal of Neurophysiology* **39**, 512–531.

Winterson, B.J. & Robinson, D.A. (1975). Fixation by the alert but solitary cat. *Vision Research* **15**, 1349–1352.

Zahs, K.R. & Stryker, M.P. (1988). Segregation of ON and OFF afferents to ferret visual cortex. *Journal of Neurophysiology* **59**, 1410–1429.